An extended-MHD model for peeling-ballooning stability thresholds in spherical tokamaks

A. Kleiner[1], N. M. Ferraro[1], G.P. Canal[2], A. Diallo[1], A. Kirk[3], L. Kogan[3], R. Maingi[1], J.T. McClenaghan[4], S.F. Smith[3]

[1] *Princeton Plasma Physics Laboratory, Princeton, NJ 08543, United States*

[2] *Instituto de Física, Universidade de São Paulo, São Paulo CEP 05508-090, Brazil*

[3] *CCFE Culham Science Centre, Abingdon, Oxon, OX14-3DB, United Kingdom*

[4] *General Atomics, San Diego, CA 92186-5608, United States*

The formation of the edge pedestal in H-mode operation is connected with periodic sudden relaxations of the edge pressure gradient, which are termed edge localized modes (ELMs). These instabilities cause expulsion of particles and heat [1] towards the plasma facing components, which can cause serious damage in reactor-scale devices. The peeling-ballooning (PB) model associates ELMs with macroscopic magnetohydrodynamic (MHD) instabilities, where (higher-n) ballooning modes are driven by the large pressure gradient and peeling modes (low-n) by the bootstrap current at the edge pedestal [2, 3]. These modes are typically considered to arise from ideal-MHD, and the model predictions well agree with experiments in large-aspect ratio machines, for example DIII-D. However, a long-standing problem has been the reliable modeling of such edge stability boundaries in spherical tokamaks (STs), where ideal-MHD models can predict stability for ELMing discharges [4]. We show that resistive peeling ballooning modes exists in a large parameter space in ELMing NSTX discharges and that resistivity can considerably expand the unstable domain, whereas discharges in ELM-free NSTX scenarios are located close to an ideal ballooning limit.

Linear stability computations are carried out with the extended-MHD code M3D-C1 [5]. In this work we seek to study the impact of plasma resistivity, gyroviscosity and equilibrium rotation, for which two-fluid terms can be neglected. Plasma resistivity is calculated according to the Spitzer resitivity model. We take the limit of ideal-MHD to be at 10% of Spitzer resistivity. This is justified as the growth rate remains nearly unchanged as resistivity is lowered further. For the presented (single fluid) simulations the same simple model of diamagnetic stabilization as in ELITE [6] is adopted. For the exact physical model used in this study we point to Ref. [7]. The stability simulations are based on kinetic equilibrium reconstructions of ELMing and ELM-free NSTX discharges (standard H-mode and wide-pedestal H-mode (WP H-mode)). The VARYPED tool is

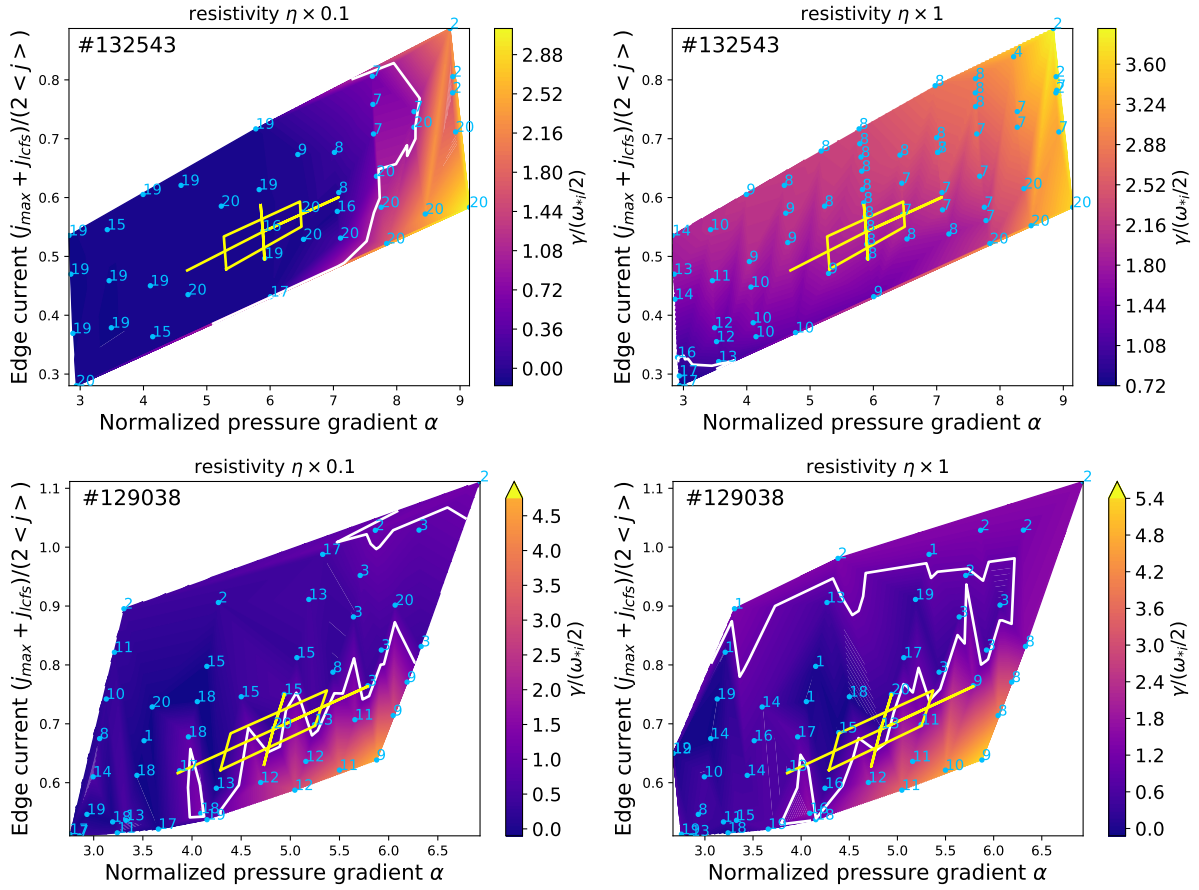

Figure 1: Peeling-ballooning stability boundary and normalized growth rate $\gamma/(\omega_{*i}/2)$ of the most unstable mode calculated for an ELMing NSTX discharge (top) and for an ELM-free WP H-mode discharge (bottom) in the ideal-MHD limit (left) and with Spitzer resistivity (right). The numbers denote the most unstable toroidal mode at each location, and the solid lines represent the stability boundary at $\gamma/(\omega_{*i}/2) = 1$.

used to scale pedestal pressure and current density, such that the plasma stored energy as well as n_e/T_e^2 are kept constant. The resistivity profile is calculated for each such equilibrium as a function of the varied T_e profile. More information on the discharges and equilibrium reconstruction/variation can be found in Ref. [7].

Fig. 1 shows the effect of plasma resistivity on the PB stability boundary in one ELMing standard H-mode NSTX discharge and in one WP H-mode discharge. The growth rates are calculated in the ideal-MHD limit and with the resistive model. When plasma resistivity is introduced a domain of unstable resistive PB modes appears [8]. This shifts the stability boundary considerably to lower values of α and j such that the experimental point appears on the unstable side consistent with the occurrence of ELMs. A shift of the stability threshold with resistivity is also seen for other considered ELMing discharges [7]. In WP H-

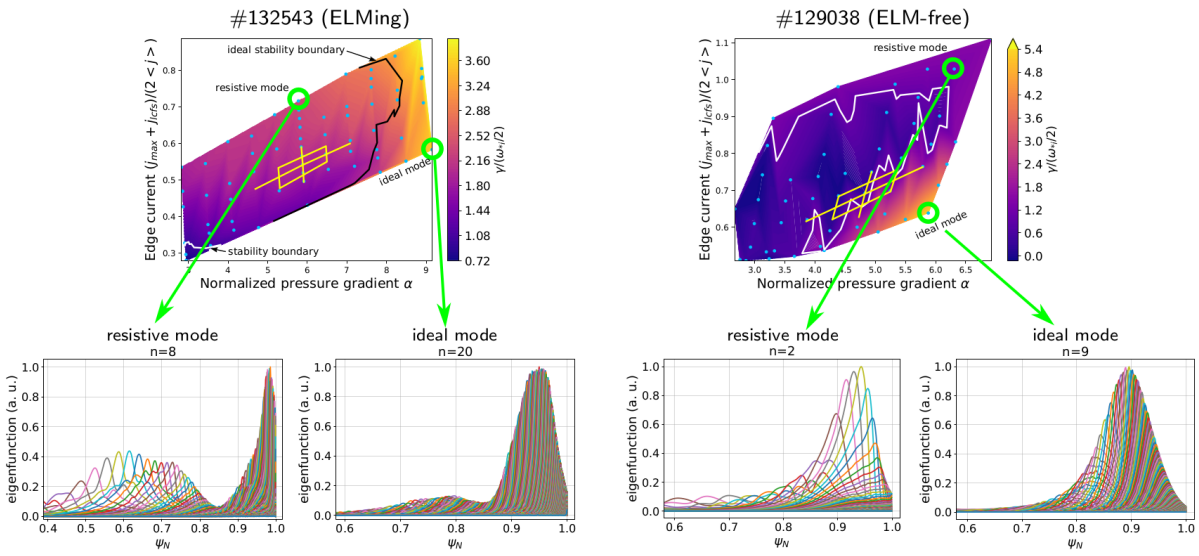

Figure 2: Poloidal spectrum of modes on the resistive kink-peeling side and in the ideal ballooning domain. (left) for ELMing discharge 132543. (right) for ELM-free WP H-mode discharge 129038. The eigenfunction of the most unstable mode is shown at the locations indicated by green circles.

mode no shift of the stability threshold close to the operational point is seen as resistivity is introduced, contrary to ELMing cases.

To better understand the differences between resistive and ideal PB modes in NSTX, we now analyze the structure of these modes in terms of their eigenfunction $\xi \propto \delta p = p(t>0) - p(t=0)$. The left hand side of Fig. 2 shows the poloidal spectrum of the most unstable toroidal mode at two locations: in the region of ideal instability at large values of α and in the region of resistive instability at moderate values of α and large values of edge current j. The ideal mode shows dominant edge ballooning mode features, i.e. it is a predominantly internal perturbation with a peak inside the pedestal. On the contrary, the resistive modes are not only current-driven since the growth rate scales with j, but also peak near the last closed flux surface indicating an external kink / peeling mode.

Besides resistivity, we also included gyroviscous stress in the calculations. The study found that gyroviscosity has a moderate stabilizing effect and can result in more accurate stability thresholds [7]. While ideal-MHD PB stability calculations in conventional aspect ratio devices are typically carried out without plasma equilibrium rotation, it is not clear if this is also true for resistive PB modes in low-aspect ratio plasmas. it is found that equilibrium rotation most notably suppresses ideal-MHD modes located in the core, and thus helps isolate edge modes. A considerable effect on PB stability cannot be inferred at

realistic values of resistivity.

In summary, robust resistive peeling-ballooning modes [8] are found well before the ideal stability threshold is met in ELMing discharges. In contrast, ELM-free discharges in NSTX are limited by ideal ballooning modes. Plasma resistivity is seen to destabilize the kink-peeling components, but not the ballooning components. Finite Larmor radius effects affect the stability limits moderately and can explain experimental access to some ELMing regimes. Based on these extended-MHD calculations ELMing discharges are correctly predicted to be unstable, whereas ELM-free plasmas remain inside the stable domain. An analysis of the resistive scaling has been performed for an ELMing MAST discharge, and a moderate resistive scaling was found. Future work will focus on the calculation of the resistive PB stability boundary in ELMing MAST discharges. It is not yet known under which general circumstances resistivity is important for PB stability. This could be due to the geometry in spherical tokamaks or the effects of recycling, i.e. a result of Li coating. Current work is underway to identify these dependencies. This result contributes to the development of a high-fidelity predictive pedestal structure model that is applicable to a broader range of tokamaks, in particular NSTX.

Acknowledgments

This research used resources of the National Energy Research Scientific Computing Center, which is supported by the Office of Science of the U.S. Department of Energy under Contract No. DE-AC02-05CH11231. This work was supported by the U.S. Department of Energy under contracts DE-AC02-09CH11466, DE-FC02-04ER54698 and the Department of Energy early career research program.

References

[1] H. Zohm, Plasma Physics and Controlled Fusion **38**, 105 (1996).

[2] P. B. Snyder *et al.*, Physics of Plasmas **9**, 2037 (2002), https://doi.org/10.1063/1.1449463.

[3] H. R. Wilson, P. B. Snyder, G. T. A. Huysmans, and R. L. Miller, Physics of Plasmas **9**, 1277 (2002), https://doi.org/10.1063/1.1459058.

[4] A. Diallo *et al.*, Nuclear Fusion **53**, 093026 (2013).

[5] S. C. Jardin, N. Ferraro, J. Breslau, and J. Chen, Computational Science & Discovery **5**, 014002 (2012).

[6] P. Snyder *et al.*, Nuclear Fusion **51**, 103016 (2011).

[7] A. Kleiner, N. Ferraro, G. Canal, A. Diallo, and R. Maingi, Nuclear Fusion **62**, 076018 (2022).

[8] A. Kleiner, N. Ferraro, A. Diallo, and G. Canal, Nuclear Fusion **61**, 064002 (2021).